The force and contact stress on the navicular bone during trot locomotion in sound horses and horses with navicular disease

A. M. WILSON*, M. P. McGUIGAN, L. FOURACRE and L. MacMAHON

Veterinary Basic Sciences, The Royal Veterinary College, North Mymms, Hatfield, Hertfordshire, AL9 7TA UK.

Summary

Mechanical overload due to poor conformation or shoeing has been suggested to contribute to the development of navicular disease. While studies have determined the compressive force exerted on the navicular bone in normal horses, this has not been reported for horses with navicular disease. Also, the force has not been converted to stress by correction for contact area. In this study we developed a technique for the determination of the contact area between the deep digital flexor tendon and the navicular bone *in vivo*, and used a forceplate system to determine the force and stress on the bone at trot in 6 normal and eight diseased horses. The mean ± s.d. peak force and peak stress were 5.62 ± 1.45 N/kg and 2.74 ± 0.76 MPa for the normal group and 6.97 ± 1.50 N/kg and 3.07 ± 0.55 MPa for the navicular disease group. The peak force and peak stress were similar for both groups but the force and stress in the horses with navicular disease were approximately double control group values early in the stance phase. This was due to a higher force in the deep digital flexor tendon, which was attributed to a contraction of the deep digital flexor muscle in early stance in an attempt to unload the heels.

Introduction

The navicular bone is a sesamoid increasing the moment arm of the deep digital flexor tendon (DDFT) on the distal interphalangeal (DIP) joint. As a result of this role, the bone experiences a compressive force during stance. This is reflected in the bone's architecture, which shows a trabecular alignment along the orientation of the compressive force from the DDFT (Parker 1973; Schryver *et al*. 1978).

Navicular disease is a degenerative disorder that involves the navicular bone and its surrounding structures, (Pool *et al*. 1989; Wright *et al*. 1998) and results in a usually bilateral lameness characterised by a toe first landing and a shortening of the anterior phase of the stride (Stashak 1987; Wyn Jones 1988; Wright 1993). The aetiopathogenesis of the condition is uncertain and many theories have been proposed which are discussed in detail elsewhere (Doige and Hoffer 1983; Hickman 1989; MacGregor 1989; Pool *et al*. 1989; Wright and Douglas 1993; Wright *et al*. 1998). In this study, we focus on one of the

mechanical theories that proposes a mechanical overload of the navicular area leads to the changes seen in the bone and its surrounding structures (Thompson *et al*. 1991; Wright and Douglas 1993).

It is possible to determine the compressive force on the navicular bone during locomotion using a combination of kinetic and kinematic analysis and radiographic measurement of limb morphology (Bartel *et al*. 1978; Willemen *et al*. 1999). This force peaks at about 6 N/kg body mass during trot locomotion in sound Warmblood horses, and is reduced in response to a raised heel shoe (Willemen *et al*. 1999). There are, however, no equivalent values for horses with navicular disease to demonstrate if the bone force is higher in these horses.

Peak force on the navicular bone is a useful measurement for the comparison of, for instance, different shoeing practices in an individual horse (Willemen *et al*. 1999) but is of little value when considering the response of musculoskeletal tissues to their mechanical environment and predicting if mechanical overload and damage is likely. The capacity for mechanical loading of cartilage and bone is a function of the tissue deformation/applied force per unit area (stress) and the number of loading cycles imposed (Carter 1984; Nigg and Herzog 1999). If navicular disease is the result of mechanical overload of the navicular bone, one would expect the peak stress on the navicular bone and the overlying fibrocartilage to be higher in horses that develop the condition than in sound horses, and for the stress to approach the values reported in the literature as causing mechanical damage to this type of tissue. There are, however, no published values for the stress imposed on the navicular bone during physiological activity.

If the peak stress experienced by the bone was higher in horses with navicular disease this would provide strong supporting evidence for the underlying cause of the condition being a mechanical overload of the navicular bone. In this study, we test the hypothesis that the peak stress on the flexor surface of the navicular bone is higher in horses that have developed navicular disease than in similar horses that have not developed the condition.

Materials and methods

Horses

Two groups were recruited for the study. The first consisted of 6 Thoroughbred cross horses in daily ridden exercise belonging to the Household Cavalry Mounted Regiment, (mean mass 629 kg;

---

*Author to whom correspondence should be addressed.

range 560–673 kg). Clinical examination showed them all to have no signs of lameness or orthopaedic abnormality. They were all assessed to have good foot balance (an unbroken hoof pastern axis and the solar surface perpendicular to the long axis of the metacarpal bone) by a veterinary surgeon and a farrier. This group was named the 'normal group'. Prior to gait analysis, their feet were trimmed to maintain the balanced state and shod with wide web shoes fitted long and wide at the heels and pulled back at the toe.

The second group was the 'navicular disease' group and consisted of 8 horses (mean mass 541 kg: range 425–590 kg). These were all cases referred to The Royal Veterinary College's Equine Referral Hospital for participation in a study on navicular disease. All had scintigraphic (Trout *et al.* 1991; Keegan *et al.* 1996) and/or radiographic (Wright *et al.* 1998) signs of navicular disease and returned to soundness after a palmar digital nerve block and after a navicular bursal block. All horses had their feet balanced and were shod with wide web shoes to the above criteria prior to assessment. Horses were between 1/10th and 4/10ths lame when trotted in a straight line and between 2/10ths and 6/10ths lame on the inside limb on a circle.

Assessment

Lateromedial and 60° dorsoproximal palmar-distal oblique radiographs were taken of both forefeet of all horses using the method described by Park and Lebel (1987). A 30 mm long piece of copper wire was placed on the midline of the dorsal hoof wall in order to determine the magnification of the image.

Retroreflective markers were constructed from 40 mm diameter, high density, polystyrene hemispheres[1] covered in retro-reflective tape[2]. These were applied to the hoof wall approximately over the centre of rotation of the DIP joint and the centre of rotation of the metacarpophalangeal joint. Markers were applied on the lateral side of the left leg and the medial side of the right leg, using hot melt glue and a hot glue gun[3].

Horses were trotted in hand, with the handler on their right hand side, at a speed comfortable for the individual horse, along a forceplate runway within a 25 m long polythene tunnel covered in light proof material. The forceplate[4] was set in concrete at the mid length of a 6mm thick commercial conveyer belt matting runway. A 900 x 600 x 10 mm aluminium plate covered in the same rubber matting was bolted to the top of the forceplate and lay flush with the surrounding rubber matting. The forceplate signal was amplified by integral eight channel charge amplifiers, filtered through a low pass filter (6db/octave from 50 Hz) and logged at 500 samples/s, via a 12 bit AD converter, into a personal computer using software written by the authors in LabView[5]. A 3D motion analysis system (Proreflex)[6] was used to determine the position of the markers from the horses' left side at a frame rate of 240 Hz. A minimum of 6, and up to 9, foot strikes were recorded for each forelimb. Data were rejected if the horse was not judged to be moving freely at constant velocity or if the foot was placed on the edge of the forceplate.

Standard formulae were used to calculate the co-ordinates of the point of zero moment (PZM). The PZM is a theoretical point where, for the purposes of mechanical analysis of locomotion, the ground reaction force (GRF) can be considered to act (Seeherman *et al.* 1987; Wilson *et al.* 1998; Nigg and Herzog 1999). Forceplate model specific, systematic

errors in the determination of the coordinates of the PZM relative to the plate were reduced using a previously published polynomial correction (Bobbert and Schamhardt 1990). The coordinates of each PZM record were expressed relative to the foot as follows: each foot was stood on a sheet of paper and the outline of the shoe drawn. The position of each side of the foot marker where it contacted the hoof was also transferred to the paper using a device manufactured in-house. The midline of the foot was determined by folding the paper to achieve superimposition of the medial and lateral shoe outlines. The fold was taken as the dorsopalmar midline of the foot and its intersection with the toe as the coordinates 0,0. The midpoint of the line joining the marker base co-ordinates was taken as the marker centre and used to express its position relative to the centre of the toe. A spreadsheet programme (Excel)[7] was used to calculate the position of the PZM relative to the toe during stance. The values of PZM and limb vertical force for each run were then reduced to 100 time points, evenly spaced through stance, by linear interpolation (Wilson *et al.* 1998). Stance was defined as the period when the vertical GRF was greater than 50 N.

The angle of the digit was calculated from the angle that the line through the foot and MCP joint markers made with the ground. This angle was determined, along with the angle between the parts of the DDFT distal and proximal to the navicular bone, for one particular digit configuration using the lateromedial radiograph recorded during standing. The change in digit angle from that value through stance was used to determine the angle of the DDFT around the navicular bone during the stance phase. This relies on the assumption that the distal phalanx is tightly attached to the hoof with negligible movement relative to the hoof wall (Bartel *et al* 1978; Willemen *et al.* 1999). Movement at the proximal interphalangeal joint was not considered as the DDFT has no attachment at this joint and, therefore, joint movement would have little effect on the angle of the DDFT around the navicular bone. The angle between the parts of the DDFT distal and proximal to the navicular bone was also interpolated to 100 points evenly spaced through stance.

Calculation of the compressive force that the DDFT exerts on the navicular bone

The forces acting about the DIP joint during stance can be considered to approximate to a static equilibrium (Parker 1973; Bartel *et al.* 1978; van den Bogert *et al.* 1989). The moment (torque) of the forces acting to extend the DIP joint about its centre of rotation must therefore be equal to the moment of those acting to flex it (Fig 1).

Since the PZM lies dorsal to the centre of rotation of the DIP joint (Schryver *et al.* 1978; Wilson *et al.* 1998), the GRF acts to extend the DIP joint. This extending moment, which is equal to the GRF multiplied by the distance between where it acts (the PZM) and the centre of rotation of the joint (Fig 1), is balanced by an equal and opposite flexing moment provided by the DDFT. This moment is equal to the force in the DDFT multiplied by the distance between the palmar border of the navicular bone and the centre of rotation of the DIP joint (Fig 1). Moments from the extensor tendons and navicular ligaments are assumed to be small and taken as zero for this calculation (Bartel *et al.* 1978; Willemen 1997).
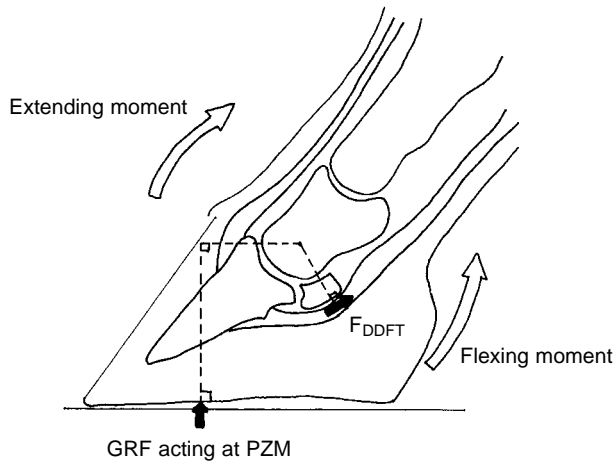
The following measurements were taken from the

Fig 1: Diagram of the forces and moment arms around the distal interphalangeal joint during stance. The ground reaction force (GRF) acts at the point of zero moment (PZM) and the extending moment that it produces is balanced by an equal and opposite flexing moment produced by the force in the deep digital flexor tendon (DDFT) and the moment arm created by the navicular bone.
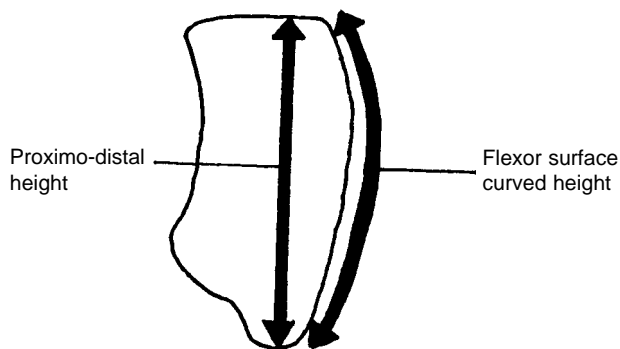

Fig 2: Measurements of proximodistal and curved height of the navicular bone taken from lateromedial radiographs. A ratio of these 2 heights was used to correct the contact area of the DDFT on the navicular bone for the curvature of the bone, in order to estimate the curved surface area of the flexor surface of the navicular bone.

lateromedial radiographs and corrected for magnification due to beam divergence using the length of copper wire on the radiograph.

1. The distance from the forward most ground bearing point of the toe to a vertical line dropped from the centre of rotation of the DIP joint. This was used to calculate the moment arm of PZM in relation to the centre of rotation of the DIP joint.

2. The distance from the centre of rotation of the DIP joint to the flexor surface of the navicular bone to give the moment arm of the DDFT force on the DIP joint.

The force in the DDFT at any point in time is, therefore, the product of limb vertical force (from the forceplate) and its moment arm (position of the PZM corrected by [1] divided by the moment arm of the DDFT [2]).

The force the DDFT exerts on the navicular bone is a function of the force in the tendon and the curvature of the

DDFT around the navicular bone, and is calculated using the following equation.

$F_{Nav} = 2[F_{DDFT} \times \cos(\alpha/2)]$
Where F_{Nav} = the compressive force on the navicular bone

F_{DDFT} = the force in the DDFT

α = the angle between the part of the DDFT proximal to the navicular bone and the part distal to it.

(Willemen 1997)

The angle α was measured along with the angle of the phalanges from the lateromedial radiographs and then corrected for the change in phalange angle during stance (as described above).

The navicular bone force data were then averaged for each individual limb and each group. Navicular bone force was also corrected for body mass to enable comparison of the horses in the different groups.

Calculation of navicular bone contact area

Six cadaveric forelimbs were sectioned at the level of the intercarpal joint and mounted in a hydraulic loading jig via a 12 mm diameter 5 cm pin drilled through the third carpal and third metacarpal bones. Each limb was compressed to a force equivalent to 30% of body weight to simulate standing. The limbs were then radiographed to obtain lateral and 60° dorsoproximal palmar-distal oblique views using the same protocol as above. A 30 mm long piece of copper wire was placed in the same plane as the navicular bone to enable correction of magnification due to beam divergence. With the limb unloaded, 5 ml of contrast medium (Urografin)[8] was injected into the navicular bursa. The limb was reloaded and radiography repeated. The bursa was flushed with the limb unloaded to remove contrast medium and 3–5 ml silicon casting material[9] injected into the bursa. This was allowed to cure for 45 min under load and 24 h in a refrigerator. The navicular bones were then dissected out with the attached casts, photographed with a scale and radiographed while laid flat on a plate with the flexor surface uppermost.

The outlines of the navicular bones from the dorsopalmar radiographs and the radiographs of the individual bones were traced onto acetate, cut out and weighed. A piece of acetate of a known area was also weighed and the data used to calculate the area of the navicular bones. The areas of the bones from the 60º dorsoproximal palmar-distal oblique view were corrected for magnification and then compared to those of the dissected bones by linear regression to produce a correction equation.

The flexor surface of the navicular bone is curved, meaning that the height on the dorso-palmar radiographs would be an underestimate of the true contact length on the flexor surface (Fig 2). The bone height (which corresponds to the maximum proximodistal height on the lateromedial radiograph) and the flexor surface contact length in that plane were determined by measurement with a piece of thread from each lateromedial radiograph as shown in Figure 2. These were expressed as a ratio for each limb and averaged to generate a multiplication factor for determination of the true navicular bone curved surface area from the 60° dorsoproximal palmar-distal radiographs.
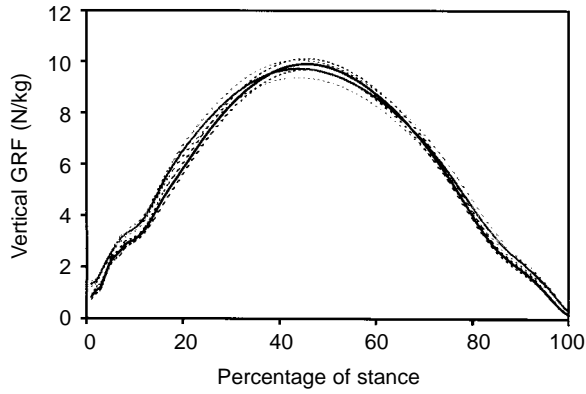
Fig 3: Graph of the vertical ground reaction force (GRF) during trot stance in normal horses - black lines and horses with navicular disease - grey lines. The dotted lines represent ± 1 s.e.
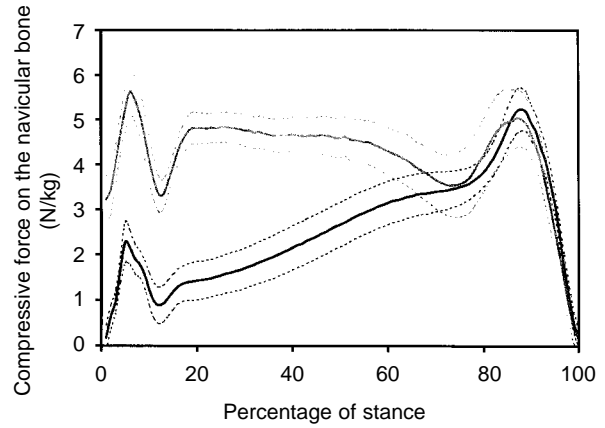

Fig 6: Graph of compressive force exerted on the navicular bone by the DDFT during trot stance in normal horses - black lines and horses with navicular disease - grey lines. The dotted lines represent ± 1 s.e.
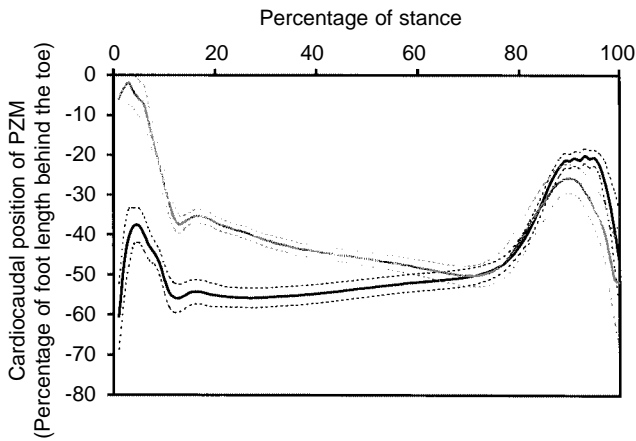

Fig 4: Graph of position of the point of zero moment during trot stance in normal horses - black lines and horses with navicular disease - grey lines. The dotted lines represent ± 1 s.e.

Fig 7: Silicon cast showing contact area between DDFT and the navicular bone.
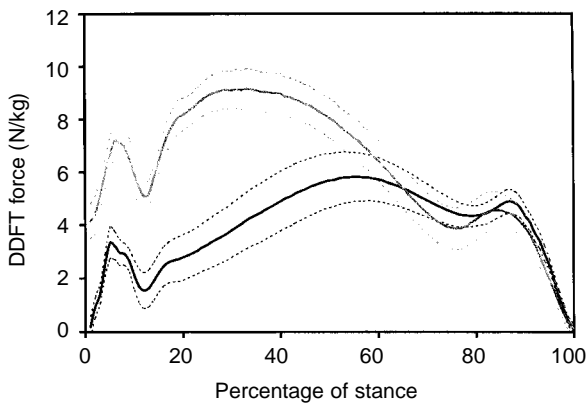

Fig 5: Graph of force in the DDFT during trot stance in normal horses - black lines and horses with navicular disease - grey lines. The dotted lines represent ± 1 s.e.
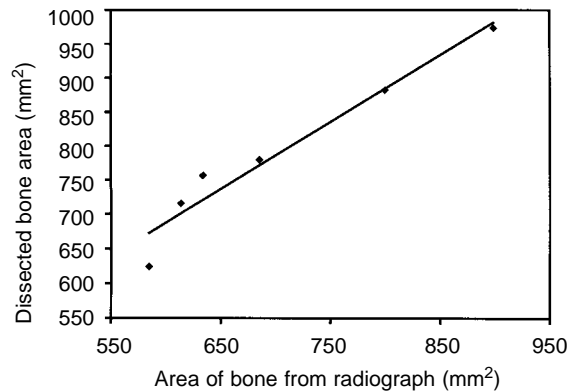

Fig 8: Graph of navicular bone area (mm^2) from the dissected bones vs. that from the 60° dorsoproximal palmar-distal oblique radiographs for the 6 legs used to calculate the correction factors. y = 0.985x+96.49, r^2=0.95
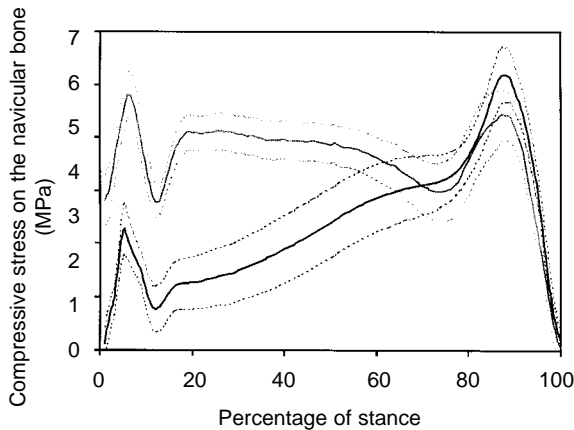
Fig 9: Graph of stress exerted on the navicular bone by the DDFT during trot stance in normal horses - black lines and horses with navicular disease - grey lines. The dotted lines represent ± 1s.e.

Calculation of the compressive stress that the DDFT exerts on the navicular bone

The navicular bone areas needed to calculate the stress imposed on the navicular bone in the 2 groups of live horses were calculated by tracing the outlines of the bones from the 60° dorsoproximal palmar-distal oblique radiographs onto over head projector film, cutting them out and weighing them. The correction and multiplication factors calculated above were then applied to obtain flexor surface contact areas. As the silicon casts indicated that the DDFT contacts the whole of the navicular bone even at low limb forces (30% body weight) we assumed that the tendon would contact the whole of the bone during stance. The compressive force on a navicular bone was then divided by the contact area of the bone to determine stress on the navicular bone through stance.

Results

Means in the text are ± s.d. and the graphs are plotted with s.e. Left and right legs were treated as independent in the analysis.

The vertical GRF time curve (Fig 3) was a similar shape in the normal and navicular disease groups and similar to that reported previously for horses at trot (Schamhardt *et al.* 1991). However, for the first 25% and the last 10% of stance, the vertical GRF was higher (s.e. do not intersect) in the navicular disease group than the normal group.

The graph of PZM during stance was different in the 2 groups (Fig 4). In the normal group there was a cranial excursion of the PZM in early stance followed by loading through most of stance at about 55% of shoe length behind the toe. The PZM started to move forward at 75–80% of stance as the heels unloaded prior to breakover. This is similar to that previously reported for normal horses (Wilson *et al.* 1998). In the navicular disease group, however, the horses landed toe first (the PZM was close to the toe) and loaded the foot in a more dorsal location until about 70% of stance. Thereafter the PZM curve was similar to that for the normal horses. The DIP joint was situated 55–75% (mean 63.5%) behind the toe, hence the more dorsal position of the PZM in the diseased group resulted in the moment arm on the DIP joint being twice that of the normal horses in early stance.

This difference in the loading pattern between the 2 groups

was also evident in the graph of DDFT force (Fig 5) which was much greater through the beginning and middle of stance in the navicular disease horses than in the normal horses. In the diseased group, the maximum DDFT force was 9.15 ± 3.04 N/kg, and this occurred at 30% of stance. The DDFT force in the normal group at this point in stance was significantly less than half this value at 4.17 ± 3.68 N/kg (P = 0.0006).

The graph of compressive force on the navicular bone during stance for the normal horses was similar in shape to that of Willemen *et al.* (1999) (Fig 6). The peak force recorded was 5.62 ± 1.45 N/kg. This plot was very different in shape for horses with navicular disease, with the initial force being much higher but the force at the end of stance being similar in magnitude to the normal horses (Fig 6). At mid stance, the values for compressive force on the navicular bone were significantly different between the 2 groups: 2.76 ± 1.67 N/kg for the normal group vs 4.52 ± 1.63 N/kg for the diseased group (P = 0.007).

Calculation of navicular bone contact area

The radiographs of the navicular bursa with contrast medium showed that most of the contrast medium was squeezed away/too thin to detect from an area approximately 20% larger than the navicular bone. The more viscous silicon casting material (which was also visible on radiographs) could be seen in thinner layers after dissection. This showed that the contact area corresponded very well with the actual area of the bone on the direct (excised) radiograph (Fig 7). We hence chose to use plain radiography of the bone rather than contrast medium to determine the contact area.

The magnification due to beam divergence on all the 60° dorsoproximal palmar-distal and lateromedial radiographs was 8%. Therefore, length measurements were divided by 1.08, and area measurements were divided by 1.08^2 to correct for this.

The areas of the dissected bones correlated well with the areas from the upright pedal radiographs (Fig 8) r^2 = 0.95. The equation of the regression line was y = 0.985x+96.49. This correction equation was applied to the areas of the bones from the 60° dorsoproximal palmar-distal radiographs. The mean curved height of the navicular bones was 1.22 times the vertical height (Fig 2) and the corrected areas were multiplied by this value to give a final navicular bone contact area.

The peak stress exerted on the navicular bone was 2.74 ± 0.76 MPa in the normal horses and 3.07 ± 0.55 MPa in the horses with navicular disease (Fig 9). These values were not significantly different. The stress at mid stance was, however, significantly different in the 2 groups: 1.19 ± 1.10 MPa for the normal horses and 1.98 ± 0.71 MPa for the navicular disease horses (P = 0.03).

Discussion

The shape of the navicular bone force-time curves were very different in the 2 populations. The normal horses showed a similar profile to that previously described by Willemen *et al.* (1999) with a gradual rise to a force peak around the time of breakover. The diseased population, however, showed a much higher force in the early part of stance which remained almost constant through to heel off. In 10 of 16 legs the highest force on the navicular bone was recorded at about 20% of stance while in all the normal legs navicular bone force peaked at around 85% of stance.

Musculoskeletal damage results from excessive peak stress,

stress rate and loading duration, (Chen *et al.* 1999). The peak stresses recorded here are 10–20% of those reported as resulting in the failure of articular cartilage and subcondral bone in a single loading cycle (Nigg and Herzog 1999; Kerin *et al.* 1998). There are no published values for the compressive failure stress of fibrocartilage. Peak limb vertical force at gallop reaches approximately 1.5 x that at trot, which should be reflected in a concomitant increase in navicular bone stress. The navicular bone and its fibrocartilage are also susceptible to fatigue damage which will be produced by smaller magnitude stresses applied repeatedly (Carter 1981; Wang *et al.* 1995).

In the calculation, an even pressure distribution on the navicular bone was presumed. Cartilage erosion usually occurs on either side of the sagital ridge (Wright *et al.* 1998) suggesting that the stress may be greater there than elsewhere on the flexor surface. The early peak in stress on the navicular bone resulted in a much higher loading rate in the navicular disease group. From Figure 9, the initial stress rate was 134 MPa/s to a stress of 2.41 MPa. The equivalent figure for the normal group was to a stress of 1.21 MPa. Chen *et al.* (1999) reported that a combination of a stress rate exceeding 30 MPa/s and a peak stress of about 2.5 MPa are required to cause cartilage damage. These criteria are met by the navicular disease group but not by the normal group. These data indicate that the navicular bone experiences stresses of a similar order to its mechanical capacity. The higher stress in early and mid stance and the higher stress rate in the navicular disease group horses perhaps accounts for the changes seen in the navicular bones of some horses with navicular disease. It would, therefore, appear possible that the gait changes in the diseased horses could result in the bone remodelling (Ostblom *et al.* 1982) and associated changes (Pool *et al.* 1989; Wright *et al.* 1998) seen in navicular disease.

The difference in the loading patterns in the 2 groups was due to an increased force in the DDFT in early and mid stance. Increased DDFT force in association with a toe first landing has previously been implicated in the development of navicular disease, (Thompson *et al.* 1991). The force in the DDFT is the sum of that created via 2 mechanisms: passive force generation via the accessory ligament and active force generation via the deep digital flexor (DDF) muscle. The force transmitted by the accessory ligament is a function of the angle of the MCP and DIP joints and rises through stance to a peak around breakover. This is believed to account for the bone force time curve of normal horses (Jansen *et al.* 1993). In normal horses, the DDF muscle exerts relatively little force during stance and lengthens through stance as the accessory ligament stretches (van den Bogert 1987).

The difference between the DDFT force time plots for the 2 groups peaked at 5.61 N/kg at 25% of stance (Fig 5). This corresponds to a difference in absolute tendon force of about 3 kN, which we suggest is generated by contraction of the DDF muscle. The DDF muscle has a pennate structure with muscle fibre lengths in the humeral head (the largest head) of about 17 mm (Hermanson and Cobb 1992). A very approximate calculation of the force generation capacity of the DDF muscle from its fibre length, its cross sectional area (2500 mm^2) and length (500 mm), reveals that it should be able to exert a peak isometric force of 3–5 kN. While the theoretical shortening of the DDF muscle is limited to about half the fibre length, i.e. 8.5 mm, the fibres will act, to some extent, in series via the sheets of aponeurosis. The DDFT was approximately 600 mm long in these horses and has an approximate force deformation response of 1500 N/% strain so it will elongate by about 12 mm with a force of 3 kN. Since there is no actual change in foot orientation

the muscle only has to account for the tendon elongation that is associated with the increase in tendon force. The DDF muscle, therefore, has the potential to generate sufficient force and length change to account for the change in tendon force seen here.

Hence, it seems probable that the increase in tendon and bone force in early stance is a result of a contraction of the DDF muscle. This also provides an explanation for the characteristic toe-first foot placement of horses with navicular disease seen here and reported in the literature (Stashak 1987; Thompson *et al.* 1991), since contraction of the DDF muscle prior to foot placement flexes the DIP joint. This muscle contraction also reduces the compliance of the digit and therefore increases the rate of vertical GRF increase (Fig 3) and loading of the navicular bone at impact. This provides an explanation for why horses with navicular disease find foot placement uncomfortable especially on hard ground even though the force on the navicular bone in normal horses peaks near the end of stance.

It is interesting that the peak force for the navicular disease horses was no higher at the end of stance. It may be that, as the force on the DDFT increases through stance, it exceeds the isometric capacity of the muscle and the muscle fibres extend transferring the DDFT force back to the accessory ligament (since DDF muscle contraction will, to some extent, unload the accessory ligament). This would return the bone force to the normal state in late stance. Without detailed individual measurements of muscle cross sectional area, pennation angle and fibre length (for instance via ultrasound) it is difficult to predict if this is the case. Alternatively, DDF muscle stimulation may be reduced after mid stance as is the case in normal horses at walk (Tokuriki *et al.* 1999).

This biomechanical response provides a possible explanation for the development of boxy feet in horses with long-standing navicular disease (Leach 1993). Contraction of the DDF muscle moves the PZM towards the toe (Fig 3) which will result in unloading of the heels. This unloading may, with time, result in contraction of the heels and a more upright hoof angle (Price and Fisher 1995). Horses with collapsed heels have been identified as being susceptible to navicular disease due to the increased passive load on the navicular bone from the DDFT, which results from the acute hoof angle (Wright and Douglas 1993). If, however, there is no pain associated with the collapsed heels then the horse will not enter the positive feedback loop and would be expected to have a relatively normal navicular bone force time plot.

It, therefore, appears that horses with navicular disease may attempt to compensate for the condition by unloading the heels via contraction of the DDF muscle. This process, however, increases the force in the DDFT and hence the compressive force exerted on the navicular bone. Why a horse would respond to pain by increasing the load on the navicular bone is unclear and counter-intuitive: perhaps other structures within the heel region are also painful in these horses, or they are unable to localise the site of pain. This may result in a positive feedback accounting for the chronic nature of the condition. A similar reaction to other heel pain would also be predicted to lead to increased loading of the navicular bone.

In conclusion, horses with navicular disease increase the load on their navicular bones in early stance, presumably due to contraction of the DDF muscle. This could lead to a positive feedback mechanism and provides a possible explanation for the progressive nature of navicular disease. Identifying and treating any concurrent causes of heel pain to break the positive feedback mechanism should therefore form part of a treatment regimen.

Acknowledgements

Manufacturers' addresses

[1]Pinflare Creative Crafts, Hertford, Hertfordshire, UK.
[2]3M, Manchester, UK.
[3]Bostik Ltd., Leicester, UK.
[4]Kistler Instrumente, AG Winterthur, CH-8408 Winterthur, Switzerland
[5]National Instruments, Newbury, Berkshire, UK.
[6]Qualisys AB, Sävedalen, Sweden.
[7]Microsoft Corporation, Redmond, Washington, USA.
[8]Schering Health Care Ltd., West Sussex, UK.
[9]RS Components, Corby, Northamptonshire, UK.

References

Bartel, D.L., Schryver, H.F., Lowe, J.E. and Parker, R.A. (1978) Locomotion in the horse: a procedure for computing the internal forces in the digit. *Am. J. vet. Res.* **39**, 1721-1727.

Bobbert, M.F. and Schamhardt, H.C. (1990) Accuracy of determining the point of force application with piezoelectric force plates. *J. Biomech.* **23**, 705-710.

van den Bogert, A.J. (1987) *Computer Simulation of Locomotion in the Horse*. PhD thesis, University of Utrecht, The Netherlands.

van den Bogert, A.J., Schamhardt, H.C. and Crowe, A. (1989) Simulation of quadrupedal locomotion using a rigid body model. *J. Biomech.* **22**, 33-41.

Carter, D.R. (1984) Mechanical loading histories and cortical bone remodeling. *Calcif. Tissue Int. Suppl.* **36**, 19-24.

Carter, D.R., Caler, W.E., Spengler, D.M. and Frankel, V.H. (1981) Uniaxial fatigue of human cortical bone. The influence of tissue physical characteristics. *J. Biomech.* **14**, 461-70.

Chen, C.T., Burton-Webster, N., Lust, G., Bank, R.A. and Tekoppele, J.M. (1999) Compositional and metabolic changes in damaged cartilage are peak-stress, stress-rate and loading-duration dependent. *J. orthop. Res*. **17**, 870-879.

Doige, C.E. and Hoffer, M.A. (1983) Pathological changes in the navicular bone and associated structures of the horse. *J. comp. Med.* **47**, 387-395.

Hermanson, J.W. and Cobb, M.A. (1992) Four forearm flexor muscles of the horse, Equus caballus: anatomy and histochemistry. *J. Morphol.* **212**, 269-280.

Hickman, J. (1989) Navicular disease – what are we talking about? *Equine vet. J.* **21**, 395-398.

Jansen, M.O., van den Bogert, A.J., Riemersma, D.J. and Schamhardt, H.C. (1993) In vivo tendon forces in the forelimb of ponies at walk, validated by ground reaction force measurements. *Acta Anat. (Basel)* **146**, 162-167.

Keegan, K.G., Wilson, D.A., Lattimer, J.C., Twardock, A.R. and Ellersieck, M.R. (1996) Scintigraphic evaluation of 99mTc-methylene disphosphonate in the navicular area of horses with lameness isolated to the foot by anesthesia of the palmar digital nerves. *Am. J. vet. Res.* **57**, 415-421.

Kerin, A.J., Wisnom, M.R. and Adams, M.A. (1998) The compressive strength of articular cartilage. *Proc. Inst. Mech. Eng. [H]* **212**, 273-80.

Leach, D.H. (1993) Treatment and pathogenesis of navicular disease ('syndrome') in horses. *Equine vet. J.* **25**, 477-481.

MacGregor, C.M. (1989) Navicular disease – in search of definition. *Equine vet. J.* **21**, 389-391.

Nigg, B.M. and Herzog, W. (1999) *Biomechanics of the Musculoskeletal System,* 2nd edn., John Riley and Sons Ltd. Chichester, England.

Ostblom, L., Lund, C. and Melsen, F. (1982) Histological study of navicular bone disease. *Equine vet. J.* **14**, 199-202.

Park, R.D. and Lebel, J.L. (1987) Equine radiography. In: *Adam's Lameness in Horses*, 4th edn., Lea and Febgier, Philadelphia. pp 188-197.

Parker, R.A. (1973) *The Analysis of the Forces and Displacements in the Digit of the Horse During Walking*. MSc Thesis, Cornell University, New York.

Pool, R.R., Meagher, D.M. and Stover, S.M. (1989) Pathophysiology of Navicular syndrome. *Vet. Clin. N. Am.: Equine Pract.* **5**, 109-129.

Price, H. and Fisher, R. (1995) *Shoeing for Performance in the Sound and Lame Horse*. The Crowood Press, Wiltshire, England.

Schamhardt, H.C., Merkens, H.W. and van Osch, G.J.V.M. (1991) Ground reaction force analysis of horses ridden at the walk and trot. In: *Equine Exercise Physiology 3*, Eds: S.G.B. Persson, A. Lindholm, and L.B. Jeffcott., ICEEP Publications, California. pp 120-127.

Schryver, H.F., Bartel, D.L., Langrana, N. and Lowe, J.E. (1978) Locomotion in the horse: kinematics and external and internal forces in the normal equine in the walk and trot. *Am. J. vet. Res.* **39**, 1728-1733.

Seeherman, H.J., Morris, E.A. and Fackelman, G.E. (1987) Computerised force plate determination of equine weight bearing profiles. In: *Equine Exercise Physiology 2*, Eds: J.R. Gillespie, and N.E. Robinson, ICEEP Publications, California. pp 536-552.

Stashak, T. (1987) *Adam's Lameness in Horses*, 4th edn., Lea and Febgier, Philadelphia. pp 499-514.

Thompson, K.N., Rooney, J.R. and Petrites-Murphy, M.B. (1991) Considerations on the pathogenesis of navicular disease. *Equine vet. Sci.* **11**, 4-8.

Tokuriki, M., Ohtsuki, R., Kai, M., Hiraga, A., Oki, H., Miyahara, Y. and Aoki, O. (1999) EMG activity of the muscles of the neck and forelimbs during different forms of locomotion. *Equine vet. J., Suppl.* **30**, 231-234.

Trout, D.R., Hornof, W.J. and O'Brien, T.R. (1991) Soft tissue- and bone-phase scintigraphy for diagnosis of navicular disease in horses. *J. Am. vet. med. Ass.* **198**, 73-77.

Wang, X.T., Ker, R.F. and Alexander, R.M. (1995) Fatigue rupture of wallaby tail tendons. *J. expt. Biol* **198**, 847-52.

Willemen, M.A. (1997) *Horseshoeing, a Biomechanical Analysis*. PhD thesis, University of Utrecht.

Willemen, M.A., Savelberg, H.H. and Barneveld, A. (1999) The effect of orthopaedic shoeing on the force exerted by the deep digital flexor tendon on the navicular bone in horses. *Equine vet. J.* **31**, 25-30.

Wilson, A.M., Seelig, T.J., Shield, R.A. and Silverman, B.W. (1998) The effect of hoof inbalance on point of force application in the horse. *Equine vet. J.* **30**, 540-545.

Wright, I.M. (1993) A study of 118 cases of navicular disease: clinical features. *Equine vet. J.* **25**, 488-492.

Wright, I.M. and Douglas, J. (1993) Biomechanical considerations in the treatment of navicular disease. *Vet. Rec.* **133**, 109-114.

Wright, I.M., Kidd, L. and Thorp, B.H. (1998) Gross, histological and histomorphometric features of the navicular bone and related structures in the horse. *Equine vet. J.* **30**, 220-234.

Wyn-Jones, G. (1988) *Equine Lameness*, Blackwell Scientific Publications, Oxford, England. pp 53-64